General Disclaimer

One or more of the Following Statements may affect this Document

- This document has been reproduced from the best copy furnished by the organizational source. It is being released in the interest of making available as much information as possible.

- This document may contain data, which exceeds the sheet parameters. It was furnished in this condition by the organizational source and is the best copy available.

- This document may contain tone-on-tone or color graphs, charts and/or pictures, which have been reproduced in black and white.

- This document is paginated as submitted by the original source.

- Portions of this document are not fully legible due to the historical nature of some of the material. However, it is the best reproduction available from the original submission.

X-681-77-255
PREPRINT

TM-78044

A SURVEY OF INTERSTELLAR HI FROM Lα ABSORPTION MEASUREMENTS II.

R. C. BOHLIN
B. D. SAVAGE
J. F. DRAKE

OCTOBER 1977

GSFC
GODDARD SPACE FLIGHT CENTER
GREENBELT, MARYLAND

A SURVEY OF INTERSTELLAR HI FROM Lα ABSORPTION MEASUREMENTS II.

R. C. Bohlin*,† B. D. Savage,*,§
and J. F. Drake‡

*Guest Investigator with the Princeton University telescope on the Copernicus satellite, which is sponsored and operated by the National Aeronautics and Space Administration.

†Goddard Space Flight Center

§Washburn Observatory, University of Wisconsin

‡Lockheed Palo Alto Research Laboratory

Submitted to Ap. J. October 1977

A SURVEY OF INTERSTELLAR HI FROM Lα ABSORPTION MEASUREMENTS II.

R. C. Bohlin*,† B. D. Savage,*,§
and J. F. Drake‡

*Guest Investigator with the Princeton University telescope on the Copernicus satellite, which is sponsored and operated by the National Aeronautics and Space Administration.

†Goddard Space Flight Center

§Washburn Observatory, University of Wisconsin

‡Lockheed Palo Alto Research Laboratory

Submitted to Ap. J. October 1977

ABSTRACT

The Copernicus satellite has surveyed the spectral region near Lα to obtain column densities of interstellar HI toward 100 stars. The distance to 10 stars exceeds 2 kpc and 34 stars lie beyond 1 kpc. Stars with color excess E(B-V) up to 0.5 mag are observed. A definitive value is found for the mean ratio of total neutral hydrogen to color excess

$$\langle N(HI+H_2)/E(B-V)\rangle = 5.8 \times 10^{21} \text{ atoms cm}^{-2} \text{ mag}^{-1}.$$

For stars with accurate E(B-V), the deviations from this mean are generally less than a factor of 1.5. A notable exception is the dark cloud star, ρ Oph, with $N(HI+H_2)/E(B-V) = 15.4 \times 10^{21}$ atoms cm^{-2} mag^{-1}. A reduction in visual reddening efficiency for the grains that are larger than normal in the ρ Oph dark cloud probably explains this result. The conversion of atomic hydrogen into molecular form in dense clouds is observed in the gas to E(B-V) correlation plots. The best estimate for the mean total gas density for clouds and the intercloud medium, as a whole, in the solar neighborhood and in the plane of the galaxy is $\langle n(HI+H_2)\rangle = 1.15$ atoms cm^{-3}; and those for the atomic gas and molecular gas alone are $\langle n(HI)\rangle = 0.86$ atoms cm^{-3} and $\langle n(H_2)\rangle = 0.143$ molecules cm^{-3}. For the intercloud medium, where molecular hydrogen is a negligible fraction of the total gas, $\langle n(HI)\rangle = 0.16$ atoms cm^{-3} with a Gaussian scale height perpendicular to the plane of about 350 pc, as derived from high latitude stars. Considerable variation in density is present at low latitudes with n(HI) ranging from <0.008 to 12 atoms cm^{-3}. Some correlation exists between neighboring directions with densities smaller than normal toward the Gum Nebula and above average in the Sco-Oph association. The general agreement and a few specific discrepancies between the Lα and 21-cm measurements of the gas are discussed.

Subject headings: abundances - interstellar matter - molecules, interstellar - spectra , ultraviolet

I. INTRODUCTION

Absorption in the HI Lα line provides a fundamental measurement of the interstellar gas. The only assumptions involved in reducing Lα profiles to column densities N(HI) are that the interstellar line has a pure damping profile and that the stellar Lα line is much narrower than the interstellar absorption. These conditions are satisfied for $N(HI) \gtrsim 5 \times 10^{18}$ cm^{-2} and for spectral types of about B2 and earlier (Savage and Panek 1974). Conversely, the 21 cm emission measurements depend on instrumental calibrations and saturation corrections. Even in the optically thin case, a model of the galactic rotation is required to obtain the spatial distribution of the gas. The neutral gas densities that are derived from 21-cm survey data apply on a galactic scale for distances greater than about 1 kpc. The stars observed in this survey at Lα are all closer than 3400pc, and two-thirds are within 1000pc. Paper I (Savage et al. 1977) contains the results for the column densities of molecular hydrogen $N(H_2) = \Sigma_J N(J)$ for 109 stars. This work (Paper II) presents N(HI) values for 100 stars, 60 of which are new measurements and 40 are from Bohlin (1975). The total hydrogen column densities $N(HI + H_2) = N(HI) + 2N(H_2)$ for the 96 stars common to Papers I and II are essential to absorption line studies of heavy element depletion for these 96 lines of sight through the interstellar medium (ISM).

II. OBSERVATIONS AND COMPARISON WITH OAO-2

The Lα region from 1170 to 1270Å was scanned at 0.2Å resolution with the U2 detector of the Copernicus satellite. Most of the U1 scans of H_2 for Paper I were obtained while U2 was moving, but still occulting the U1 stray light hole (Rogerson et al. 1973). The Lα spectra were corrected for stray and scattered light according to the prescription of Bohlin (1975). Values for N(HI) were derived by multiplying the observed spectra by exp $[+ \sigma_\lambda N(HI)]$ for various trial

values of N(HI) and then choosing the N(HI) that provided the best continuum reconstruction (see Bohlin 1975 for details). A Lorentzian profile was assumed for σ_λ, the absorption cross section. The values for N(HI) for the 40 stars from the earlier work were unchanged in this paper, with the exceptions of α Vir and ζ Cen. The upper limit for α Vir becomes the actual N(HI) because of measurements in the higher Lyman lines (York and Rogerson 1976). Because of probable stellar contamination for a B2.5 IV star, the column density for ζ Cen is now listed as an upper limit (see York 1976). The final results for all 100 stars are in Table 1, where the columns are: (1) HD number, (2) name, (3) galactic longitude and (4) latitude, (5) spectral type, (6) photometry in V and (7) B-V, (8) the color excess in B-V, (9) the stellar distance in pc, (10) the atomic hydrogen column density in atoms cm^{-2}, (11) the probable error for N(HI) in percent, (12) the mean space density of atomic hydrogen in atoms cm^{-3}, (13) the molecular hydrogen column density from Paper I in molecules cm^{-2} with the power of 10 in parentheses, (14) $N(HI+H_2) = N(HI)+2N(H_2)$, the total neutral hydrogen column density in atoms cm^{-2}, and (15) the total mean space density of hydrogen along the line of sight in atoms cm^{-3}. The sources of the spectral types and photometry and the method of computing distances are listed in Paper I. A colon indicates an uncertain value.

The second largest set of interstellar Lα spectra was obtained by OAO-2 for 95 stars and analyzed by Savage and Jenkins (1972) and Jenkins and Savage (1974). The Copernicus values for N(HI) have smaller error bars and are preferred for the 47 stars observed by both satellites. Figure 1 compares the data for the 47 stars and provides a basis for evaluating the 48 values of N(HI) determined only by OAO-2. The filled circles are from the first Copernicus survey of 40 stars (Bohlin 1975), and the open circles are new results from this paper. The open circles tend to lie at larger values of N(HI), because this second survey emphasizes more highly reddened stars. Below $N(HI)=10^{20} cm^{-2}$, the OAO-2 values are often much too large, since at 12Å resolution the OAO-2 spectra do not

distinguish the interstellar core from the dominant stellar Lα line. For $N(HI) > 10^{20}$ cm^{-2}, the two determinations rarely differ by more than expected, as shown for some typical error bars. Thus, the OAO-2 column densities are a satisfactory secondary source for individual stars, except for ζ Cas, where N(HI) from Bohlin (1973) is preferred.

III. GAS TO COLOR EXCESS RATIO

The observations divide naturally into two different groups, depending on whether the fraction of H_2, $f = 2N(H_2)/[2N(H_2) + N(HI)]$, is more or less than 1 percent. Usually, the amount of H_2 is at least a factor of 100 below 1 percent whenever it is that low because of the bimodal distribution of $N(H_2)$ found by Bohlin (1975) and Spitzer and Jenkins (1975), also see Paper I. The low and high values of f probably determine whether the line of sight is entirely in the intercloud medium, or whether it intersects a region of high density, where H_2 concentrations can be large. Table 2 contains the mean values computed from the data, where all peculiar, emission line, Wolf-Rayet stars, stars with uncertain photometry, and the 4 stars without H_2 measurements have been excluded from consideration. The upper limits on $N(H_2)$ have been set equal to zero when computing the total amounts of hydrogen, since the upper limits are less than a few percent of N(HI) in all cases. Except for the gas to color excess values, these means are not representative of the ISM, as a whole, but are typical for the lines of sight to bright OB stars.

a) Interpretation

The entry in Table 2 for $< N(HI+H_2)/E(B-V) >$ for all 75 stars provides a definitive value of 5.8×10^{21} atoms cm^{-2} mag^{-1} for the mean ratio of total neutral hydrogen to color excess E(B-V), a measure of the dust. The mean for the 30 stars

with $f < 0.01$ is in good agreement with this global average, contrary to the results of Bohlin (1975), who found a significantly lower value. This change was caused by the inclusion of new measurements and the exclusion of peculiar and emission line stars, which tend to be intrinsically reddened. The value of 5.8×10^{21} atoms cm^{-2} mag^{-1} does not include a correction for the ionized component of the ISM in HII regions. However, Jenkins (1976) has estimated that only about 4 percent of the total gas is ionized for the present set of OB stars. This is consistent with the accepted value of the mean electron density $\langle n_e \rangle = 0.03$ cm^{-3} (Taylor and Manchester 1977).

Figure 2 illustrates the good correlation between the gas and E(B-V). Figure 2a includes all 100 stars from Table 1, where the dashed line is the mean of 4.8×10^{21} cm^{-2} mag^{-1} for atomic hydrogen alone. In Figure 2b, the 96 stars with both HI and H_2 column densities scatter about the dashed line for 5.8×10^{21} cm^{-2} mag^{-1} representing the average ratio of total hydrogen to color excess. The open symbols denote the stars with uncertain E(B-V) that are omitted in calculating the mean values of Table 2. A number of these points lie to the right of the dashed line because of intrinsic reddening. The two most deviant points are for the Be stars, ϕ Per (B2 Vpe) and 59 Cyg (B1.5 Venn). If the actual interstellar reddening is average for the measured $N(HI+H_2)$, then both ϕ Per and 59 Cyg have an intrinsic (B-V) reddening of $0^m.14$. This reddening is probably the result of atmospheric extension (see Fig. 13 in Haisch and Cassinelli 1976).

In Figure 2 the conversion of hydrogen into molecular form is clearly evident for $E(B-V) > 0.2$. The scatter of the points about the mean lines is reduced in 2b and most of the deficiences of gas at large E(B-V) in 2a are removed in 2b, even though only 17 percent of the total measured gas is H_2. The triangles are the stars with mean observed densities $n(HI+H_2) > 1$ cm^{-3}. The expectation that a bigger fraction of H_2 exists in the most opaque clouds is supported by the

5 triangles at E(B-V) > 0.3 that fall the farthest below the dashed line in 2a, but are located normally in 2b. The slight tendency for the triangles to lie higher than the circles in 2b might be caused by a change in the shape of the extinction curves in dense clouds due to a conversion of small grains into larger ones (see the discussion for ρ Oph in § IIIc). Below E(B-V) = 0.04, the deviation of the filled circles from the dashed line is probably not significant because of the errors in the estimates of E(B-V). For $0.04 \leq E(B-V) \leq 0.08$, there are 7 filled circles in Figure 2b which seem to lie systematically low. Part of this effect may be due to general ionization in the Gum Nebula (see IV) and in the stellar HII regions. The closest HII regions suffer the greatest fractional ionization in the line of sight. Since 4 of these 7 stars are iota and the 3 belt stars in Orion, another possible contribution is anomalous reddening in that part of the sky.

b) Independent Determinations

Table 3 summarizes the modern measurements of the gas to color-excess ratio, using independent techniques. All values for both the atomic and total gas are in excellent agreement. For E(B-V) > 0.10 where the photometry errors are minor, the internal agreement of the individual stars in Figure 2b is also excellent, with a typical scatter of only ∿30 percent about the mean line. Rarely does a point differ by more than a factor of 1.5 from 5.8×10^{21} cm^{-2} mag^{-1}. Thus, for most of the diffuse interstellar medium, $\langle N(HI+H_2)/E(B-V) \rangle$ seems to be a constant, independent of location in the sky. However, the point for ρ Oph suggests that this ratio is different for stars with anomalous extinction (see § IIIc).

The 21-cm measurements summarized in Table 3 are toward distant globular clusters and stars with known E(B-V). Over the same range as Figure 2 in E(B-V), the same result for $\langle N(HI)/E(B-V) \rangle$ is obtained from all three sources. If the

galactic dust distribution is thinner than that of the gas, as suggested by FitzGerald (1968), the gas to color-excess ratio should be larger at high latitudes. However, neither the present data, nor the results of Knapp and Kerr (1974), nor those of Heiles (1976) show convincing evidence for a systematic variation of the ratio with galactic latitude. The interpretation of the 21-cm results is complicated at low latitudes and at high E(B-V), because of conversion of atomic gas to molecular form and possible saturation of the 21-cm line emission (Knapp and Kerr 1974).

X-ray absorption occurs over a large range in extinction for supernova remnants with E(B-V) < 1.5, and up to E(B-V) = 9.5 toward the galactic center. The X-ray absorption is primarily due to HI, H_2, and the elements carbon, nitrogen, and oxygen. The reduction to equivalent hydrogen atoms requires the assumption of universal ratios of elemental abundance. Although the X-ray value for the gas to color excess includes the ionized component of the ISM, the mean ionization fraction cannot be derived from the difference between the X-ray and the ultraviolet results, because the ratio of heavy elements to hydrogen is more uncertain than the 15 percent difference between 5.8 and 6.7 x 10^{21} cm^{-2} mag^{-1}. In fact, the abundance of heavy elements probably increases toward the galactic center (Peimbert et al. 1977, Churchwell et al. 1977).

c) ρ Ophiuchi

The point for ρ Oph A in Figure 2b deviates significantly from the trends exhibited by the other stars. The value of $N(HI+H_2)/E(B-V) = 15.4 \times 10^{21}$ cm^{-2} mag^{-1} is a factor of 2.7 larger than the mean interstellar ratio. The HI and H_2 data for this star are of high quality and the color excess, E(B-V) = 0.47, appears reliable; therefore, this discrepancy is real. Variations in the gas to E(B-V) ratio can be produced by actual changes in the gas to dust mass ratios or by changes in the shape of the interstellar extinction curve, and hence, changes in the dust scattering and absorbing efficiency between the B and V bandpasses. Carrasco, Strom, and Strom (1973) have presented evidence for an increase in the average particle size for the dust in the densest regions of the ρ Ophiuchi dark cloud. Of those stars in Table 1 that lie in the ρ Ophiuchi cloud, ρ Oph A appears to have the most anomalous extinction characteristics. The wavelength of maximum linear polarization peaks near 6900 Å rather than at the interstellar average of 5450 Å (Serkowski, Mathewson, and Ford 1975). The color-excess ratios E(V-K)/E(B-V) and E(V-L)/E(B-V) of 3.59 and 3.55 (Carrasco et al. 1973) imply a value of $R = A_V/E(B-V)$ significantly larger than the interstellar average of 3.1. Finally, the far ultraviolet extinction curve for ρ Oph AB does not exhibit the rapid rise toward short wavelengths that characterizes the average interstellar curve (Bless and Savage 1972). These extinction results imply that the grains toward ρ Oph are larger than for normal interstellar regions and it appears likely that the anomalous gas to E(B-V) ratio for ρ Oph is the result of the peculiar shape of the extinction curve for this star. The large grains that are required to explain a larger than normal R are inefficient in producing visual reddening. Therefore, if the total gas to dust mass ratio is nearly normal, an increase in $N(HI+H_2)/E(B-V)$ would be expected for any region containing a significant excess in the relative numbers of large particles.

IV. GALACTIC DISTRIBUTION OF HI

The best estimate of the mean gas density in the galactic plane is derived from the product of the average gas to color excess ratio of 5.8×10^{21} cm^{-2} mag^{-1} and the mean color excess per kpc of 0.61 mag kpc^{-1} for matter in the plane (Spitzer 1968). The result is

$$\langle n(HI+H_2) \rangle = 1.15 \text{ atoms cm}^{-3}.$$

From Paper I, $\langle n(H_2) \rangle = 0.143$ molecules cm^{-3}, which applies to matter in the plane within 500pc of the sun, and may be only a lower limit because of selection effects. Consequently, the best value for

$$\langle n(HI) \rangle = 0.86 \text{ atoms cm}^{-3}$$

might be an overestimate. Gordon and Burton (1976) derive $\langle n(HI+H_2) \rangle = 1.2$ cm^{-3} at 10 kpc from the galactic center, in agreement with our value. They used 21-cm data to derive $\langle n(HI) \rangle = 0.4$ cm^{-3} and CO observations and a series of uncertain corrections to deduce $\langle n(H_2) \rangle = 0.4$ cm^{-3}. Detailed comparisons of the results from the two techniques are dangerous, because the radio data applies to the mean for a ring of the ISM located at a galactocentric distance of 10 kpc, while the Copernicus measurements are of the solar neighborhood. Both sets of mean densities could be exactly correct because they refer to different volumes of space.

The location in the galactic coordinates of each star in this survey is at the center of one of the ellipses in Figure 3. The width of each ellipse is proportional to the distance to the star and the height represents the mean HI space density (or its upper limit). Thus, the area of an ellipse is proportional to N(HI). In the ideal situation, it would be valuable to know the gas density n(x,y,z) at every point in the solar neighborhood. The Lα data determine only the mean density n(HI) along certain lines of sight which are non-randomly selected. The main selection effects are that the O3 stars tend to lie near the galactic

plane and that the stars tend to exist in groups or associations. Three of these well known associations are indicated in Figure 3, where 21-cm measurements show an excess of gas in two of them, Per and Sco-Oph (Sancisi 1970, 1974). On the other hand, the limiting observation distance for Copernicus is a strong function of the reddening. Thus, the densest concentrations of gas cannot be sampled at all, resulting in a general under-sampling of regions with an excess or even a normal amount of gas.

Despite these limitations, Figure 3 contains much information on the nature of n(x,y,z). Since a uniform interstellar medium would show ellipses of the same height where the width increases with distance, short ellipse represents a lower than average space density, and a tall ellipse shows a high n(HI). Figure 3 demonstrates that the local density is strongly inhomogeneous. However, neighboring stars tend to have about the same mean density, particularly if they are close in distance. A striking example is the large region near the galactic plane centered at $\ell \sim 250^{\circ}$, where the Gum Nebula is located (see Savage and Jenkins 1972, Bohlin 1975, and Brandt et al. 1976). The ellipses are all short out to distances beyond 1000pc. Occasionally, stars about 100 pc away like υ and λ Sco have little gas in the line of sight compared to more distant stars in neighboring directions. The apparent continuity of the distribution in Figure 3 suggests that the unsampled regions of the solar neighborhood have an N(HI) that could be estimated from the closest survey star in 3 dimensions. Outside of the dense Per and Sco-Oph clouds, the only significant exception is the pair HD 54662 and 55879 near $\ell = 225^{\circ}$ and $b = -1^{\circ}$, which are with 2° in angle and 20 percent in distance, but differ by a factor of 4 in n(HI), and also $n(HI+H_2)$. Even though an approximate spatial correlation exists in Figure 3, the best technique for estimating $N(HI+H_2)$ for an arbitrary direction is to use the average gas to color excess ratio and the extensive maps of E(B-V) as a function of ℓ, b, and r in FitzGerald (1968).

Observations in the EUV below 912 Å are limited to directions where N(HI) is very low, because of absorption in the Lyman continuum (Cruddace et al. 1974). If the density distribution is spatially coherent, as suggested above, the upper limits on N(HI) toward β and ε CMa indicate that atomic hydrogen column densities may be $<10^{19}$ cm^{-2} over a 10-40° region out to 200 pc. According to the cross sections of Cruddace, et al. (1974), this implies an optical depth τ less than unity shortward of about 200 Å. However, longer wavelengths are still inaccessible. At 600 Å, τ=1 for N(HI) = 5×10^{17} cm^{-2}, which corresponds to a distance of 1 pc for the mean density of 0.16 cm^{-3}, or just 16 pc at the low value of n(HI) = 0.01 cm^{-3}.

Because of the large extinction at ultraviolet wavelengths (Stecher 1969 and Bless and Savage 1972), the limiting distance for observations at Lα is a strong function of E(B-V). Figure 4 helps assess the effects of this incomplete sampling to a given distance for the Copernicus data. The total hydrogen column density for 96 stars is shown as a function of the stellar distance. Dashed lines represent the average density of 0.16 cm^{-3} for the intercloud stars (stars with $f < 0.01$; see Table 2) and the derived overall average of 1.15 cm^{-3} for the gas in the plane within 1000 pc of the sun. The filled symbols denote stars with $f < 0.01$, and the open symbols indicate stars with $f > 0.01$. The circles refer to high latitude stars, where $b > 10^{\circ}$ and $z = r \sin|b| > 60$ pc. The triangles are the low latitude stars with $b \leq 10^{\circ}$ or $z \leq 60$ pc. Because of the good correlations between the gas and E(B-V), the strong effect of the reddening on the ultraviolet flux produces a cutoff in the observed $N(HI+H_2)$ at about 2×10^{21} cm^{-2}, almost independent of the distance. Only ρ Oph, with its anomalous extinction, has $N(HI+H_2)$ significantly greater than 2×10^{21} cm^{-2}. The mean line n = 1.15 cm^{-3} for matter in the plane within 1000pc of the sun is not representative of the observations. The reason for this is that the average reddening of the observed stars is below the average reddening of 0.61 mag kpc^{-1} for matter in the plane (Spitzer 1968), so that most of the observed

column densities are less than the average, at all distances. Those few nearby stars that do lie above the mean line for $n = 1.15$ cm^{-3} are in Sco-Oph association where there is an excess of gas.

The filled symbols for the low H_2 stars in Figure 4 scatter about the lower mean line for the intercloud stars with $n = 0.16$ cm^{-3}. This indicates that the selection effects for this subset of directions is not large and, therefore, a density of 0.16 cm^{-3} is probably typical for regions of the ISM where there are no dense clouds containing significant amounts of H_2. Baker and Burton (1975) derive $n = 0.17$ cm^{-3} for the intercloud hydrogen using their spherical cloud model, where there are 3 clouds kpc^{-1} with a diameter of 5 pc and column densities of 3×10^{20} cm^{-2}. The tendency for the nearest stars to fall below the $n = 0.16$ cm^{-3} line is mainly indicative of the general ionization in the direction of the Gum Nebula. Only for $r > 1000$ pc do the open and filled circles (high latitude stars) fall systematically below their corresponding set of triangles (low latitude stars), as expected when the line of sight falls appreciably out of the thin galactic gas layer.

If $n(HI) = 0.16$ cm^{-3} is the correct intercloud density in the galactic plane, the scale height h for this component of the ISM can be estimated for a Gaussian density distribution of gas in the z direction, perpendicular to the plane where

$$n(z) = 0.16 \exp\left(\frac{-z^2}{2h^2}\right) \text{ cm}^{-3}. \qquad (1)$$

Provided the z velocity distribution of the gas is Gaussian, a Gaussian distribution for n(z) would be expected, since the gravitational acceleration in the z direction varies approximately linearly with distance above the plane (Oort 1960). The 8 lines of sight with $|b| > 30^0$ provide the best measure of the z-distribution, since low latitude stars may be contaminated by the selection of stars in associations. A ninth star HD219188 with $b = -50^0$ does not provide a pure sample of the intercloud medium, because 6 percent of the hydrogen is molecular. The 8 high latitude

observations are shown with error boxes in Figure 5, where

$$N(z) \approx N(HI) \sin|b| \qquad (2)$$

for a plane parallel stratification of gas. The measurement for α Vir should not be given much weight because of possible small scale density fluctuations or significant ionization in this short line of sight. Baker and Burton (1975) give h = 120 pc for the intercloud gas and about the same density $n = 0.17\ cm^{-3}$ in the plane for this component. However, the integral of equation (1) $N(z) = \int_0^z n(z')\,dz'$ for h = 120 pc does not fit the data well. A much more extended distribution of gas is indicated with h closer to 350 pc. With an exponential density distribution given by

$$n(z) = 0.16 \exp\left(-\frac{z}{h}\right) cm^{-3},$$

the data are fitted reasonably well with h = 500 pc. Jenkins (1978) found a roughly similar exponential scale height, h = 300 (+200, -150) pc, for interstellar OVI.

The HI Lα data do not suggest any asymmetries above and below the plane, but 2 of the 5 most distant stars in Figure 5 are toward the galactic anticenter and lie below the other 3 stars which are within 90^0 of the galactic center. Thus, the Lα data shows weak evidence for an increasing scale height toward the center of the galaxy. The new generations of ultraviolet telescopes in orbit should provide a more definitive determination of n(z) using the same technique discussed here.

V. DISCUSSION OF THE Lα MEASUREMENTS IN COMPARISON TO 21-CM DATA

As discussed earlier, the general comparison of the results of the ultraviolet survey do not conflict with the gross properties of the gas inferred from observations at 21-cm. In fact, the overall value for $\langle n(HI+H_2)\rangle = 1.15\ cm^{-3}$ and $n = 0.16\ cm^{-3}$ for the intercloud gas in the plane agree well with the values derived from radio data. A more detailed comparison, star by star, does not reveal an entirely

satisfactory picture. Observations at 21-cm with the radio telescope centered on stars of interest provide the best comparison and have been obtained by Habing (1968), Goldstein and MacDonald (1969), Grayzeck and Kerr (1974), Giovanelli et al. (1978), and Cram (personal communication). The observations of Habing were made with a large beam size (37' by 40'), while Goldstein and MacDonald have calibration uncertainties. Because of these problems and significant improvements in radio receivers in recent years, the data obtained in the 1960's will not be considered here. The column densities deduced by Grayzeck and Kerr are based on absolute measurements of brightness temperature, which should be accurate to $\pm$ 5 percent (Harten, et al. 1975).

At low galactic latitudes, much of the gas may lie beyond the star, so that the only interesting cases are where N(HI) > N(21-cm). For values of N(21-cm) from Grayzeck and Kerr, this condition is true for several stars, including δ Sco (Bohlin 1975). However, the Grayzeck and Kerr baselines systematically differ from those adopted by Giovanelli et al. (1978) and Cram. In general, high velocity wings up to $\sim$100 km s^{-1} that are seen by Giovanelli et al. and Cram make their column densities larger than those found by Grayzeck and Kerr. Differences in calibration are probably present, also. For example, Cram finds an N(21-cm) more than a factor of 2 greater than that of Grayzeck and Kerr for ω^1 Sco. In this case, the difference in baseline accounts for only about 20 percent of the total discrepancy.

The only unambiguous case were N(HI) > N(21-cm) is for ρ Oph with the preliminary value for the column density from Cram of more than a factor of three below the Lα result. Thus, the vitiated discussion for δ Sco in Bohlin (1975) still applies for ρ Oph. Either small dense clouds in the 21-cm beam or large optical depths suggested by the low value of 46K for the excitation temperature of H_2 from Paper I may explain the low 21-cm signal. In addition, the 21-cm profile should be examined for high velocity wings. A high resolution spatial and velocity mapping with the 21' beam used to observe ρ Oph by Cram would be a useful investigation with the VLA.

At high galactic latitudes, a comparison between N(HI) and precision 21-cm data would provide a measure of any tenuous HI in distant parts of the galactic halo. For stars at z > 500 pc, Figure 5 demonstrates that N(HI) should equal N(21-cm) for a Gaussian distribution with a reasonable scale height. Unfortunately, the 21-cm data toward high latitude stars is less accurate than at low latitudes. The 21-cm survey of about 200 OB stars (Cram personal communication) is the only survey that includes most of the stars observed at Lα. Of the three stars at $|b| > 30^{o}$ observed by both Cram and Giovanelli et al., two agree well, but their values for HD93521 differ by more than a factor of three. This discrepancy results in part from different velocity coverage, but also points out the increased difficulty of assigning the proper baseline at high latitudes because of 21-cm radiation from the galaxy in the far sidelobes of the 140' antenna used for both measurements. In addition, the near sidelobes are important. Therefore, to unambiguously determine cloud sizes and reduce antenna temperatures to column densities, a full mapping of a large region around the stars is essential in order to make the spatial deconvolution of the beam pattern. A high resolution mapping is necessary because the distribution of gas over much of the sky at high latitudes show extensive structure on a scale comparable to typical 21-cm beam sizes (eg. see Fejes and Verschuur 1973). Reliable 21-cm column densities toward high latitude stars are very difficult or, perhaps, impossible to obtain with single dish antennas. Thus, Lα absorption measurements may provide the best source of information on the tenuous neutral gas in the galactic halo.

Discussions with T. Cram, R. Giovanelli, F.J. Kerr, and D. York clarified the problems associated with the interpretation of 21-cm data. Comments from E. Jenkins, L. Spitzer, and T. Stecher produced a significant improvement in the final manuscript. T. Snow cheerfully transmitted the large amounts of Copernicus data to GSFC on a regular basis, while K. Feggans was reponsible for

the initial data processing at Goddard. B. D. S. acknowledges partial support through NASA grants NSG 5100 and NSG 5181, and J. F. D. was supported by the Lockheed Independent Research Program.

REFERENCES

Baker, P. L., and Burton, W. B. 1975, Ap. J., 198, 281

Bless, R. C., and Savage, B. D. 1972, Ap. J., 171, 293.

Bohlin, R. C. 1973, Ap. J., 162, 139.

Bohlin, R. C. 1975, Ap. J., 200, 402.

Brandt, J. C., Roosen, R. G., Thompson, J., and Ludden, D. L. 1976, Ap. J., 208, 109.

Carrasco, L., Strom, S. E., and Strom, K. M. 1973, Ap. J., 182, 95.

Churchwell, E., Smith, L. F., Mathis, J., Mezger, P. G., Huchtmeier, W. 1977, Astron. and Astrophys., in press.

Cruddace, R., Paresce, F., Bowyer, S., and Lampton, M. 1974, Ap. J., 187, 497.

Fejes, I., and Verschuur, G. L. 1973, Astron. and Astrophys., 25, 85.

FitzGerald, M. P. 1968, A. J., 73, 983.

Giovanelli, R., Haynes, M. P., York, D. G., and Shull, J. M. 1978, Ap. J., Jan. 1.

Goldstein, S. J., and MacDonald, D. D. 1969, Ap. J., 157, 1101.

Gordon, M. A., and Burton, W. B. 1976, Ap. J., 208, 346.

Gorenstein, P. 1975, Ap. J., 198, 95.

Grayzeck, E. J., and Kerr. F. J. 1974, A. J., 79, 368.

Habing, H. J. 1968, Bull. Astr. Inst. Netherlands, 20, 120.

Haisch, B. M., and Cassinelli, J. P. 1976, Ap. J., 208, 253.

Harten, R. H., Westerhout, G., and Kerr, F. J. 1975, A. J., 80, 307.

Heiles, C. 1976, Ap. J., 204, 379.

Jenkins, E. B., and Savage, B. D. 1974, Ap. J., 187, 243.

Jenkins, E. B. 1976, in The Structure and Content of the Galaxy and Galactic Gamma Rays, eds. C. E. Fichtel and F. W. Stecker (NASA-GSFC, X-662-76-154.)

Jenkins, E. B. 1978, Ap. J., (in press).

Knapp, G. R., and Kerr, F. J. 1974, Astr. and Ap., 35, 361.

Oort, J. H. 1960, B.A.N., 15, 45.

Peimbert, M., Torres-Peimbert, S., and Rayo, J. F. 1977, "Abundance Gradients in the Galaxy Derived from HII Regions," preprint.

Rogerson, J. B., York, D. G., Drake, J. F., Jenkins, E. B., Morton, D. C., and Spitzer, L. 1973, Ap. J. (Letters), 181, L110.

Ryter, C., Cesarsky, C. J., and Audouze, J. 1975, Ap. J., 198, 103.

Sancisi, R. 1970, Astr. and Ap., 4, 387.

Sancisi, R. 1974, in Galactic Radio Astronomy, Eds. F. J. Kerr and S. C. Simonson, Proceedings of IAU, 115.

Savage, B. D., Bohlin, R. C., Drake, J. F., and Budich, W. 1977, Ap. J., 216, 291, (Paper I).

Savage, B. D., and Jenkins, E. B. 1972, Ap. J., 172, 491.

Savage, B. D., and Panek, R. J. 1974, Ap. J., 191, 659.

Serkowski, K., Mathewson, D. S., and Ford, V. L. 1975, Ap. J., 196, 261.

Spitzer, L. 1968, Diffuse Matter in Space (New York: Wiley).

Spitzer, L., and Jenkins, E. B. 1975, Ann. Rev. Astr. and Ap., 13, 133.

Stecher, T. P. 1969, Ap. J. Lett., 157, L125.

Taylor, J. H., and Manchester, R. N. 1977, Ap. J., 215, 885.

York, D. G. 1976, Ap. J., 204, 750.

York, D. G., and Rogerson, J. B. 1976, Ap. J., 203, 378.

R. C. BOHLIN: NASA Goddard Space Flight Center, Code 681, Greenbelt, MD 20771.

J. F. DRAKE: Department 52-10/B202, Lockheed Palo Alto Research Laboratory, 3251 Hanover Street, Palo Alto, CA 94304.

B. D. SAVAGE: Department of Astronomy, Sterling Hall, University of Wisconsin, Madison, WI 53706.

TABLE 1

ATOMIC AND MOLECULAR HYDROGEN COLUMN DENSITIES

HD	NAME	l	b	S.T.	V	B-V	E(B-V)	r (pc)	N(HI) (10^{20} cm^{-2})	Error (%)	n(HI) (cm^{-3})	$N(H_2)$ (cm^{-2})	N(HI + H_2) (10^{20} cm^{-2})	n(HI + H_2) (cm^{-3})
(1)	(2)	(3)	(4)	(5)	(6)	(7)	(8)	(9)	(10)	(11)	(12)	(13)	(14)	(15)
886	γ Peg	109	-47	B2 IV	2.84	-.23	.01	145	1.1	20	.25	<1.6(14)	1.1	.25
2905	κ Cas	121	0	B1 Ia	4.17	+.13	.35	1009	16.	30	.51	1.88(20)	19.8	.64
5394	γ Cas	124	-2	B0.5 IVpe	2.68	-.20	(.08)	194	1.45	20	.24	<3.2(17)	1.45	.24
10516	ϕ Per	131	-11	B2 Vpe	4.09	-.04	(.20)	137	3.5	20	.83	.12(20)	3.7	.88
14633		141	-18	ON8 V	7.45	-.21	.10	2042	3.0	30	.057	<.13(20)	3.0	.057
21856		156	-17	B1 V	5.89	-.07	.19	681	11.0	20	.01	1.10(20)	13.2	.74
22951	40 Per	159	-17	B1 IV	4.96	-.02	.24	406	11.0	30	.88	2.9(20)	16.8	1.34
23180	o Per	160	-18	B1 III	3.79	+.06	.30	230	8.0	30	1.09	4.0(20)	16.1	2.2
24398	ζ Per	162	-17	B1 Ib	2.87	+.11	.33	394	6.4	10	.53	4.7(20)	15.8	1.30
24760	ϵ Per	157	-10	B0.5 III	2.90	-.18	.08	308	2.6	20	.26	.33(20)	3.2	.33
24912	ξ Per	160	-13	O7.5 IIInf	4.03	+.01	.32	638	13.0	20	.78	3.4(20)	19.8	1.20
28497		209	-37	B1.5 Ve	5.60	-.23	.02	466	1.60	20	.111	6.6(14)	1.60	.111
30614	α Cam	144	14	O9.5 Ia	4.29	+.02	.32	1164	8.0	20	.22	2.2(20)	12.4	.34
34989		166	-16	B1 V	5.79	-.13	.13	603	13.0	20	.70	<.028(20)	13.	.70
35149	23 Ori	169	-18	B1 Vn	4.99	-.15	.11	429	5.5	20	.42	<.034(20)	5.5	.42
36486	δ Ori	204	-18	O9.5 II	2.23	-.23	.07	384	1.70	20	.144	4.8(14)	1.70	.144
36822	ϕ^1 Ori	195	-13	B0.5 IV-V	4.41	-.17	.11	413	6.5	20	.51	.21(20)	6.9	.54
36861	λ Ori	195	-12	O8 IIIf	3.39	-.19	.12	532	6.0	25	.37	.132(20)	6.3	.38
37043	ι Ori	210	-20	O9 III	2.77	-.24	.07	429	1.40	15	.106	4.9(14)	1.40	.106
37128	ϵ Ori	205	-17	B0 Ia	1.70	-.19	.08	409	2.8	20	.22	3.7(16)	2.8	.22
37202	ζ Tau	186	-6	B2 IVp	2.95	-.19	.05	145	1.10	20	.25	<4.7(17)	1.10	.25
37742	ζ Ori	206	-17	O9.7 Ib	1.77	-.21	.08	352	2.6	20	.24	5.4(15)	2.6	.24
38666	μ Col	237	-27	O9.5 V	5.16	-.29	.01	701	0.70	20	.032	3.2(15)	0.70	.032
38771	κ Ori	215	-19	B0.5 Ia	2.09	-.18	.07	520	3.3	10	.21	4.6(15)	3.3	.21
40111	139 Tau	184	1	B1 Ib	4.83	-.07	.15	1247	8.0	20	.21	.54(20)	9.1	.24
44743	β CMa	226	-14	B1 II-III	1.97	-.24	.00	206	<.05	-	<.008	<2.0(17)	<.05	<.008
47129		206	0	O8 p	6.06	+.05	.35	752	12.0	50	.52	3.5(20)	19.0	.82
47839	15 Mon	203	2	O7 Vf	4.65	-.25	.07	705	2.5	20	.115	3.5(15)	2.5	.115
48099		206	1	O7 V	6.35	-.05	.27	1169	14.0	40	.39	1.95(20)	17.9	.50
50896		235	-10	WN 5 + B	6.84:	-.25	.14	1393	3.5	30	.081	0.20(20)	3.9	.091
52089	ϵ CMa	240	-11	B2 II	1.50	-.20	.01	188	<.05	-	<.009	<4.6(17)	<.059	<.010
53138	o^2 CMa	236	-8	B3 Ia	3.04	-.10	.04	1009	1.50	20	.048	-	-	-
53975		226	-2	O7.5 V	6.47	-.10	.22	1334	14.0	20	.34	.170(20)	14.3	.35
54662		224	-1	O6.5 V	6.21	+.03	.35	1236	24.	30	.63	1.00(20	26.	.68
55879		225	0	B0 III	6.04	-.18	.10	1462	8.0	30	.177	<.08(20)	8.0	.177
57060	29 CMa	238	-5	O7 Ia:fp	4.9:	-.14	.18	1871	5.0	20	.087	6.0(15)	5.0	.087
57061	τ CMa	238	-6	O9 II	4.40	-.16	.15	933	5.0	10	.174	3.0(15)	5.0	.174
57682		224	3	O9 IV	6.40	-.19	.12	1614	7.4	20	.149	<.09(20)	7.4	.149
58350	η CMa	243	-6	B5 Ia	2.46	-.08	.02	759	.70	20	.030	-	-	-
66811	ζ Pup	256	-5	O4 Inf	2.26	-.28	.04	668	.97	5	.047	2.8(14)	.97	.047
68273	γ^2 Vel	263	-8	O9 I + WC8	1.83	-.26	.05	377	.60	10	.052	1.70(14)	.60	.052
74375		276	-11	B1.5 III	4.32	-.12	.10	348	6.6	20	.62	<.022(20)	6.6	.62
91316	ρ Leo	235	53	B1 Iab	3.85	-.14	.08	959	1.80	20	.061	4.1(15)	1.80	.061
92740		287	-1	WN7	6.41	+.08	.33	2780	16.0	30	.187	.93(20)	17.9	.21
93030	o Car	290	-5	B0.5 Vp	2.76	-.22	.06	207	1.90	20	.30	<4.5(17)	1.90	.30
93521		183	62	O9 Vp	7.04	-.28	.03	1778	1.30	30	.024	<.035(20)	1.30	.024
99171		286	17	B2 IV-V	6.11	-.19	.05	470	4.5	20	.31	1.80(15)	4.5	.31
112244		304	6	O8.5 Iaf	5.36	+.03	.34	1854	12.0	20	.21	1.38(20)	14.8	.26
113904	o Mus	305	-2	O9 II	5.50	-.02	.29	1276	12.0	20	.30	.68(20)	13.4	.34
116658	α Vir	316	51	B1 IV	0.97	-.26	.03	86	0.100	25	.038	8.9(12)	0.100	.038

TABLE 1 (continued)

HD	NAME	l	b	S.T.	V	B-V	E(B-V)	r (pc)	N(HI) (10^{20} cm^{-2})	Error (%)	n(HI) (cm^{-3})	N(H_2) (cm^{-2})	N(HI + H_2) (10^{20} cm^{-2})	n(HI + H_2) (cm^{-3})
(1)	(2)	(3)	(4)	(5)	(6)	(7)	(8)	(9)	(10)	(11)	(12)	(13)	(14)	(15)
121263	ξ Cen	314	14	B2.5 IV	2.54	-.24	0	85	<1.05	-	<.40	6.3(12)	<1.05	<.40
122451	β Cen	312	1	B1 III	0.62	-.24	.00	84	.33	10	.127	6.3(12)	.33	.127
136501		320	-3	O7.5 IIIf	5.43	-.09	.22	1178	12.0	30	.33	.59(20)	13.2	.36
141637	1 Sco	340	22	B1.5 Vn	4.63	-.05	.20	232	16.5	20	2.2	.170(20)	15.8	2.2
143018	π Sco	347	20	B1 V + B2	2.90	-.18	.08	171	5.2	10	.09	.21(20)	6.0	1.06
143275	δ Sco	350	23	B0.5 IV	2.33	-.12	.10	155	14.0	20	2.9	.26(20)	14.5	3.0
144217A	β^1 Sco	353	24	B0.5 V	2.63	-.08	.20	161	12.4	10	2.5	.67(20)	13.7	2.8
144470	ω^1 Sco	353	23	B1 V	3.94	-.04	.22	227	15.0	20	2.1	1.13(20)	17.3	2.5
145502	ν Sco	355	23	B2 IVp	4.01	+.03	.27	174	14.0	40	2.6	.78(20)	15.6	2.9
147165	σ Sco	351	17	B1 III	2.9	+.14	.38	142	22.	40	6.0	.61(20)	23.2	6.3
147933	ρ Oph A	354	18	B2 IV	4.61	+.23	.47	174	65.	20	12.1	3.7(20)	72.	13.5
148184	χ Oph	358	21	B1.5 Ve	4.43	+.28	.53	134	14.0	20	3.4	4.3(20)	22.0	5.5
148605	22 Sco	353	16	B2 V	4.78	-.14	.10	217	9.0	20	1.35	.055(20)	9.1	1.36
149038	μ Nor	339	3	O9.7 Iab	4.89	+.09	.38	1122	10.0	20	.29	2.8(20)	15.6	.45
149438	τ Sco	352	13	B0 V	2.84	-.24	.06	236	3.1	10	.43	3.2(14)	3.1	.43
149757	ζ Oph	6	24	O9.5 Vnn	2.56	+.02	.32	138	6.2	5	1.22	4.4(20)	14.1	3.3
149881		31	36	B0.5 III	6.0 Var	-.14:	.12	1614	4.5	40	.090	<.1(20)	4.5	.090
150898		339	-8	B0.5 Ia	5.57	-.07	.18	2323	9.0	20	.126	.04(20)	10.3	.143
151804		344	2	O8 Ief	5.47	+.09	.40	1795	12.0	30	.22	1.80(20)	15.6	.28
152408		344	1	O8:Iafpe	5.82:	+.17	.48	1888	18.0	30	.31	2.4(20)	22.8	.39
155806		353	3	O7.5 Vnn	5.52	+.01	.33	736	12.0	30	.53	.84(20)	13.7	.60
157246	γ Ara	335	-11	B1 Ib	3.33	-.14	.08	689	4.8	20	.23	.170(20)	5.1	.24
158408	ν Sco	351	-2	B2 IV	2.70	-.22	.02	134	<.18	-	<.043	<1.3(14)	<.18	<.043
158926	λ Sco	352	-2	B1.5 IV	1.63	-.22	.03	102	<.24	-	<.076	5.0(12)	<.24	<.076
164353	67 Oph	30	13	B5 Ib	3.97	+.02	.12	762	10.0	40	.43	1.83(20)	13.7	.58
164402		7	0	B0 Ib	5.84	+.01	.28	1738	13.0	20	.24	.31(20)	13.6	.25
165024	θ Ara	343	-14	B2 Ib	3.66	-.08	.10	745	7.0	20	.30	<.09(20)	7.0	.30
167263	16 Sgr	11	-2	O9.5 II-IIIn	5.98	+.01	.31	1349	12.0	30	.29	1.52(20)	15.0	.36
167264	15 Sgr	10	-2	B0 Ia	5.38	+.07	.34	1656	14.0	30	.29	1.90(20)	17.8	.37
175191	σ Sgr	10	-12	B3 IV	2.09	-.20	.00	67	<.30	-	<.17	<1.0(14)	<.30	<.17
184915	κ Aql	32	-13	B0.5 IIIn	4.96	-.01	.20	630	8.0	30	.41	2.05(20)	12.1	.62
186994		79	10	B0.2 IV	7.56	-.29:	0:	2365	8.0	40	.110	<.44(20)	8.0	.110
188001	9 Sge	56	-4	O7.5 Iaf	6.25	+.01	.33	2831	11.0	30	.126	-	-	-
188209		81	10	O9.5 Iab	5.65	-.09	.21	2014	8.0	30	.129	1.02(20)	10.0	.162
188439		82	10	B0.5 IIIn	6.30	-.12	.14	1358	6.0	40	.143	0.90(20)	7.8	.186
193322AB		78	3	O9 V:n	5.82	+.09	.40	608	12.0	40	.64	1.20(20)	14.4	.77
193924	α Pav	341	-35	B2.5 V	1.94	-.20	.02	57	<.20	-	<.11	<2(14)	<.20	<.11
199579		86	0	O6 Vf	5.96	+.04	.36	1086	12.0	40	.36	2.3(20)	16.6	.50
200120	59 Cyg	88	1	B1.5 Vunn	4.79	-.07	.18	257	1.80	20	.23	.20(20)	2.2	.28
203064	68 Cyg	88	-4	O7.5 III:nf	5.01	-.03	.28	893	10.0	30	.36	1.98(20)	14.0	.51
204172	69 Cyg	83	-10	B0 Ib	5.94	-.10	.17	2118	10.0	30	.153	.40(20)	10.8	.165
209975	19 Cep	105	5	O9.5 Ib	5.12	+.08	.38	1086	13.0	30	.39	1.20(20)	15.4	.46
210191	35 Aqr	37	-52	B2.5 IV	5.74	-.15:	.07:	336	<4.6	-	<.44	<.04(20)	<4.7	<.44
210839	λ Cep	104	3	O6 Infp	5.06	+.24	.56	991	13.0	20	.42	6.0(20)	25.	.82
214080		46	-57	B1 Ib	6.80	-.14	.08	3404	4.4	40	.042	<.1(20)	4.4	.042
214680	10 Lac	97	-17	O9 V	4.88	-.20	.11	589	5.0	30	.28	.165(20)	5.3	.29
215733		85	-36	B1 II	7.2	-.21:	.03:	3034	5.0	40	.053	-	-	-
218376	1 Cas	110	-1	B0.5 III	4.84	-.04	.22	621	9.0	30	.47	1.40(20)	11.8	.62
219188		83	-50	B0.5 II-IIIn	6.93	-.18:	.09:	2365	7.0	40	.096	.22(20)	7.4	.102
224572	σ Cas	116	-6	B1 V	4.89	-.09	.17	377	7.5	20	.65	1.70(20)	10.9	.94

TABLE 2

OBSERVATIONAL AVERAGES

	30 "intercloud" stars f<0.01	45 "cloud" stars f>0.01	all 75 stars
$\langle n(HI) \rangle = \frac{\Sigma N(HI)}{\Sigma r}$ (atoms cm^{-3})	0.16	0.44	0.35
$\langle n(H_2) \rangle = \frac{\Sigma N(H_2)}{\Sigma r}$ (molecules cm^{-3})	<0.001	0.053	0.036
$\langle n(HI+H_2) \rangle = \frac{\Sigma[N(HI)+2N(H_2)]}{\Sigma r}$ (atoms cm^{-3})	0.16	0.55	0.42
$\langle E(B-V)/r \rangle = \frac{\Sigma E(B-V)}{\Sigma r}$ (mag kpc^{-1})	0.10	0.28	0.22
$\langle r \rangle = \frac{\Sigma r}{\text{no. of stars}}$ (pc)	620	870	770
$\langle N(HI)/E(B-V) \rangle = \frac{\Sigma N(HI)}{\Sigma E(B-V)}$ (atoms cm^{-2} mag^{-1})	5.0×10^{21}	4.8×10^{21}	4.8×10^{21}
$\langle N(HI+H_2)/E(B-V) \rangle = \frac{\Sigma[N(HI)+2N(H_2)]}{\Sigma E(B-V)}$ (atoms cm^{-2} mag^{-1})	5.0×10^{21}	5.9×10^{21}	5.8×10^{21}

TABLE 3

GAS TO COLOR EXCESS RATIO

(10^{21} atoms cm^{-2} mag^{-1})

	UV Spectra	21-cm	X-ray*
$\langle N(HI)/E(B-V)\rangle$	4.8	4.85(A), 5.1 (B)	———
$\langle N(HI+H_2)/E(B-V)\rangle$	5.8	———	6.6(C), 6.8(D)

*The mean X-ray result of 6.7 x 10^{21} $cm^{-2}s^{-1}$ includes the ionized component of the ISM. The two individual results are both average values for a few supernova remnants and the galactic center X-ray source.

A Heiles (1976)

B Knapp and Kerr (1974)

C Gorenstein (1975)

D Ryter, et al. (1975)

FIGURE CAPTIONS

Fig. 1 - Comparison between the Lα column densities obtained by Copernicus (OAO-3) and those from OAO-2. The dashed line is the locus of points representing exact agreement. The filled circles are from Bohlin (1975) and the open circles are the stars from the present survey.

Fig. 2 - (a) shows the correlation between the atomic hydrogen column density N(HI) and E(B-V), while (b) shows the correlation between the total hydrogen column density, $N(HI+H_2) = N(HI) + 2N(H_2)$, and E(B-V). In both (a) and (b), the dashed lines are the average ratios from Table 2. The triangles are the stars with high mean densities, $n(HI+H_2) > 1$ atom cm^{-3}; and the circles represent cases where $n(HI+H_2) < 1$ atom cm^{-3}. Open symbols denote stars with uncertain E(B-V) that were omitted in calculating the mean ratios.

Fig. 3 - The measured amount of atomic hydrogen as a function of ℓ , b , and r. Each star is located at the center of an ellipse, whose width is proportional to the stellar distance. The mean density n(HI) is proportional to the height of the ellipse, while the area is a measure of the column density N(HI). The representation for the total neutral gas is quite similar. Three prominent OB associations are labeled.

Fig. 4 - The total gas column density, $N(HI+H_2)$, as a function of stellar distance. The upper dashed line represents the derived mean $n(HI+H_2) = 1.15$ atoms cm^{-3} for matter in the plane. The lower dashed line is the mean $n(HI+H_2) = 0.16$ atoms cm^{-3} for the intercloud medium (see Table 2). Filled symbols denote stars with $f < 0.01$. Open symbols denote stars with $f \geq 0.01$. Circles denote stars with $|b| > 10^{o}$ and $z > 60$pc. Triangles denote stars with $|b| \leq 10^{o}$ or $z \leq 60$pc.

Fig. 5 - $N(z) = N(HI) \sin|b|$ verses the distance z above the plane of the galaxy. The error boxes denote the observations with $\pm 0^{m}.5$ allowed for the uncertainty in the absolute stellar magnitudes from which distances are estimated. The solid curves are the theoretical values of N(z) for a plane-parallel distribution in z with a density of 0.16 cm^{-3} in the plane. Two values of the scale height h for the assumed Gaussian distribution are shown.

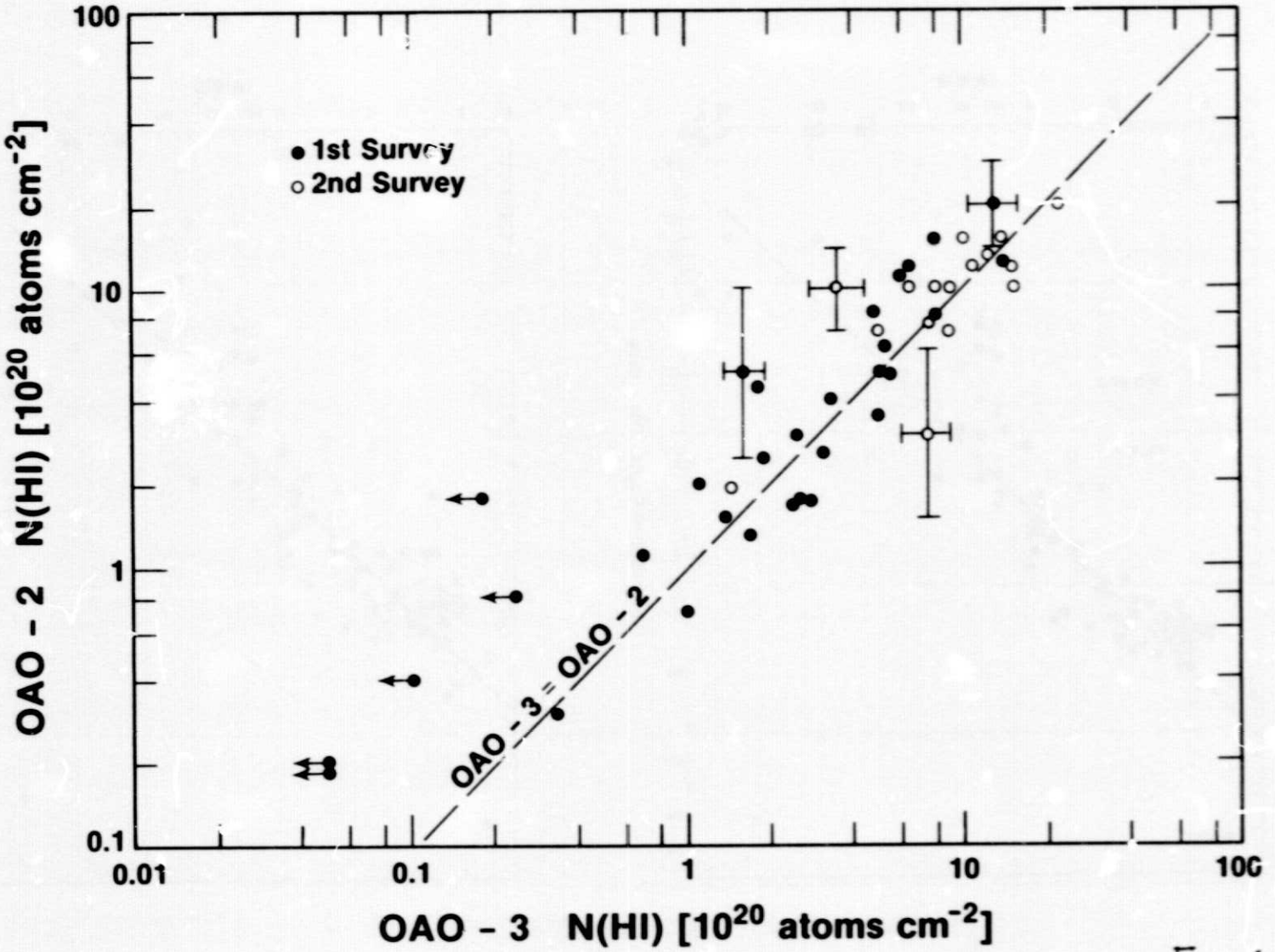
100
10
1
0.1
0.01
0.1
1
10
100
● 1st Survey
○ 2nd Survey
OAO - 3 = OAO - 2
OAO - 2 N(HI) [10^20 atoms cm^-2]
OAO - 3 N(HI) [10^20 atoms cm^-2]

Fig. 1

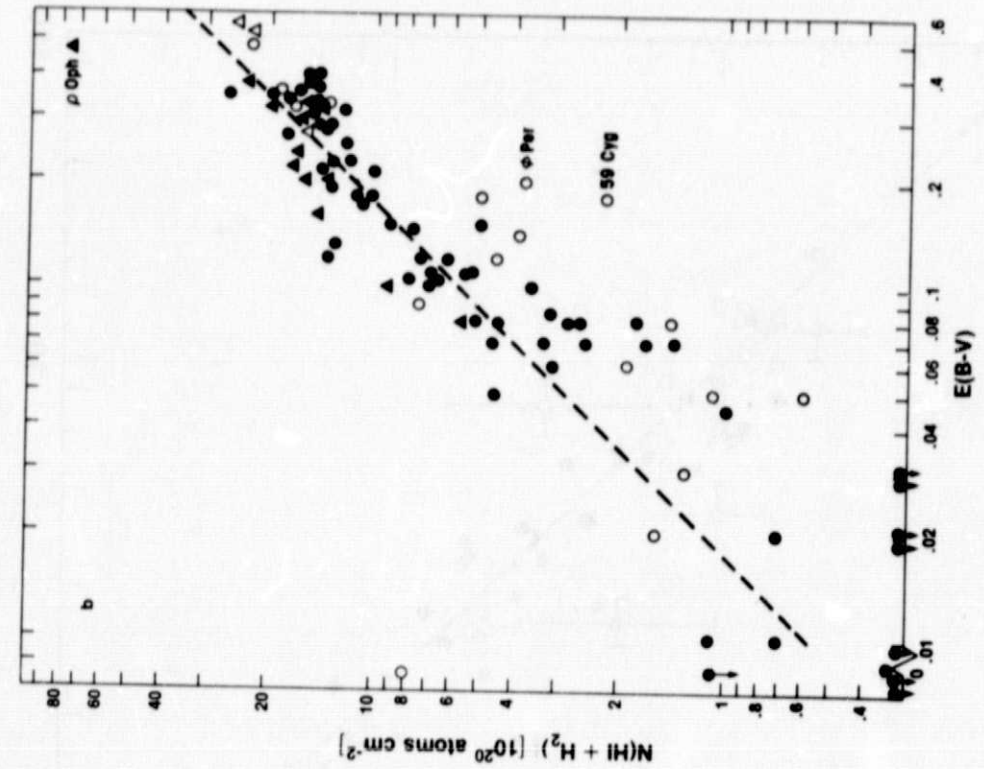

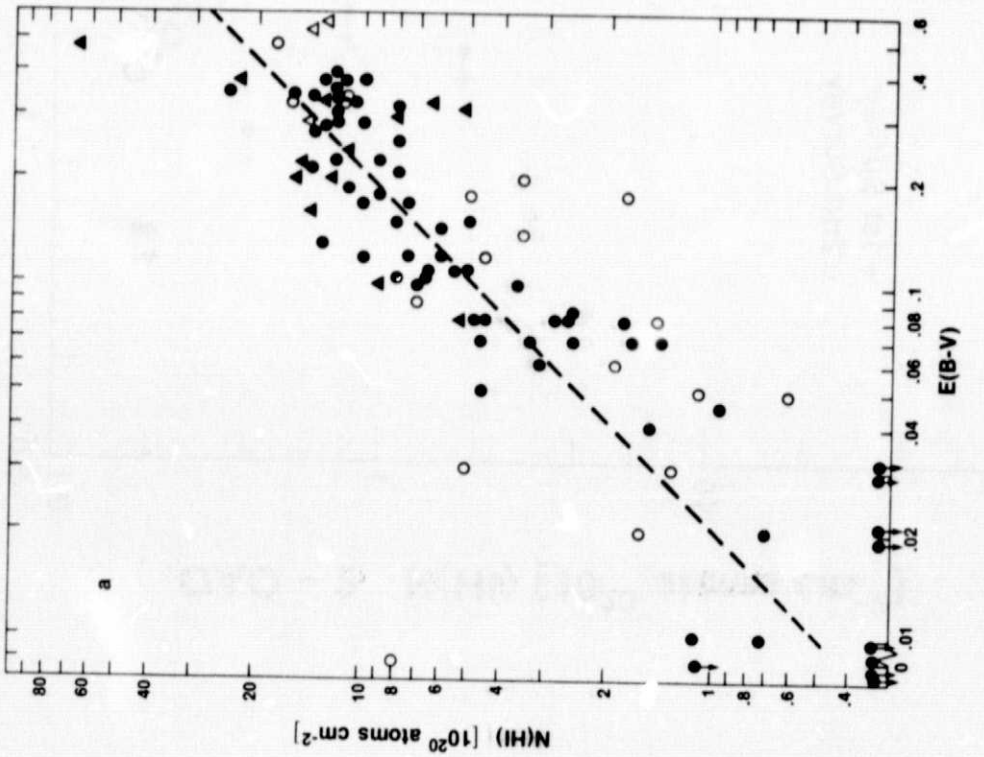

Fig 2.

Fig. 3

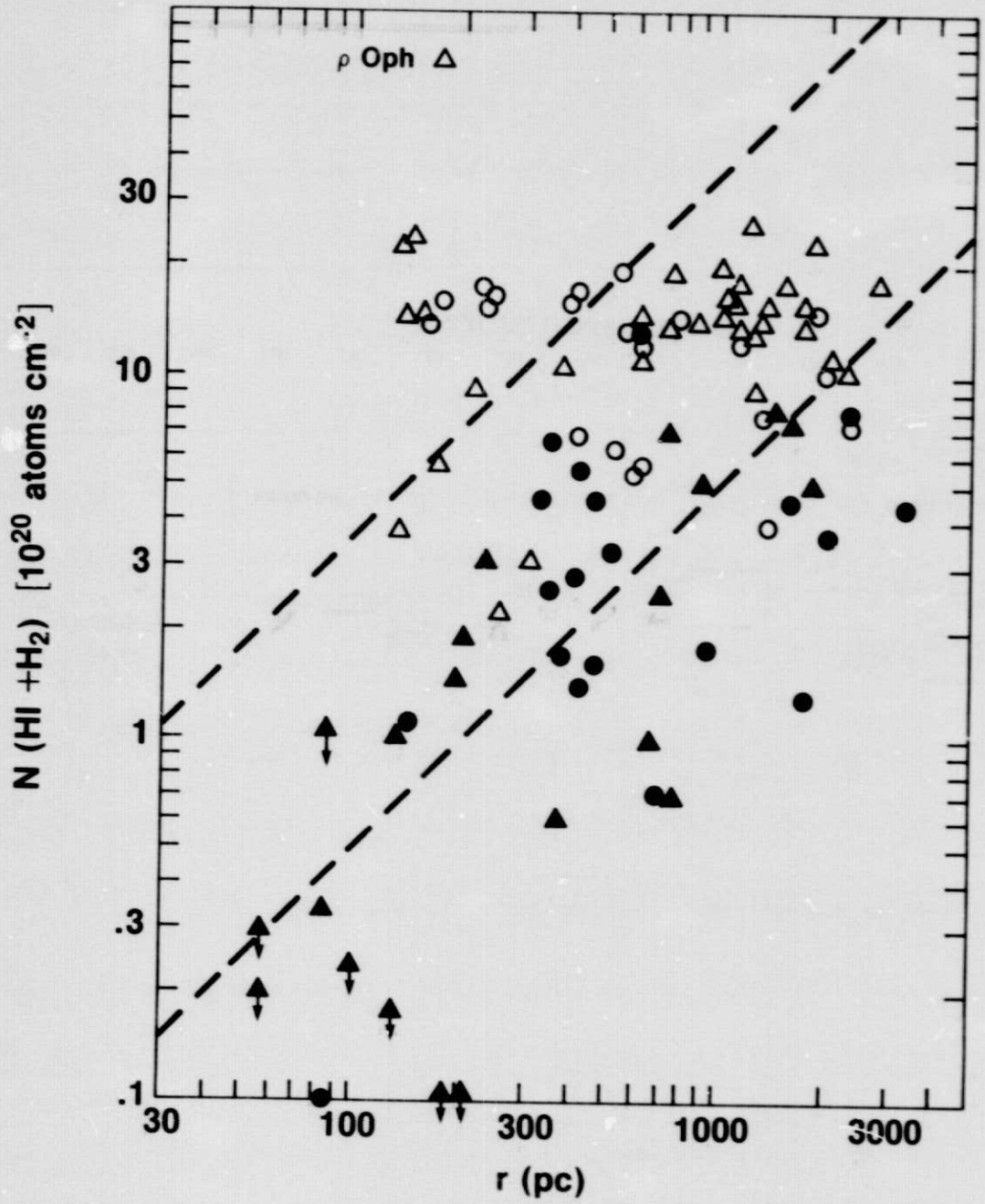

Fig. 4

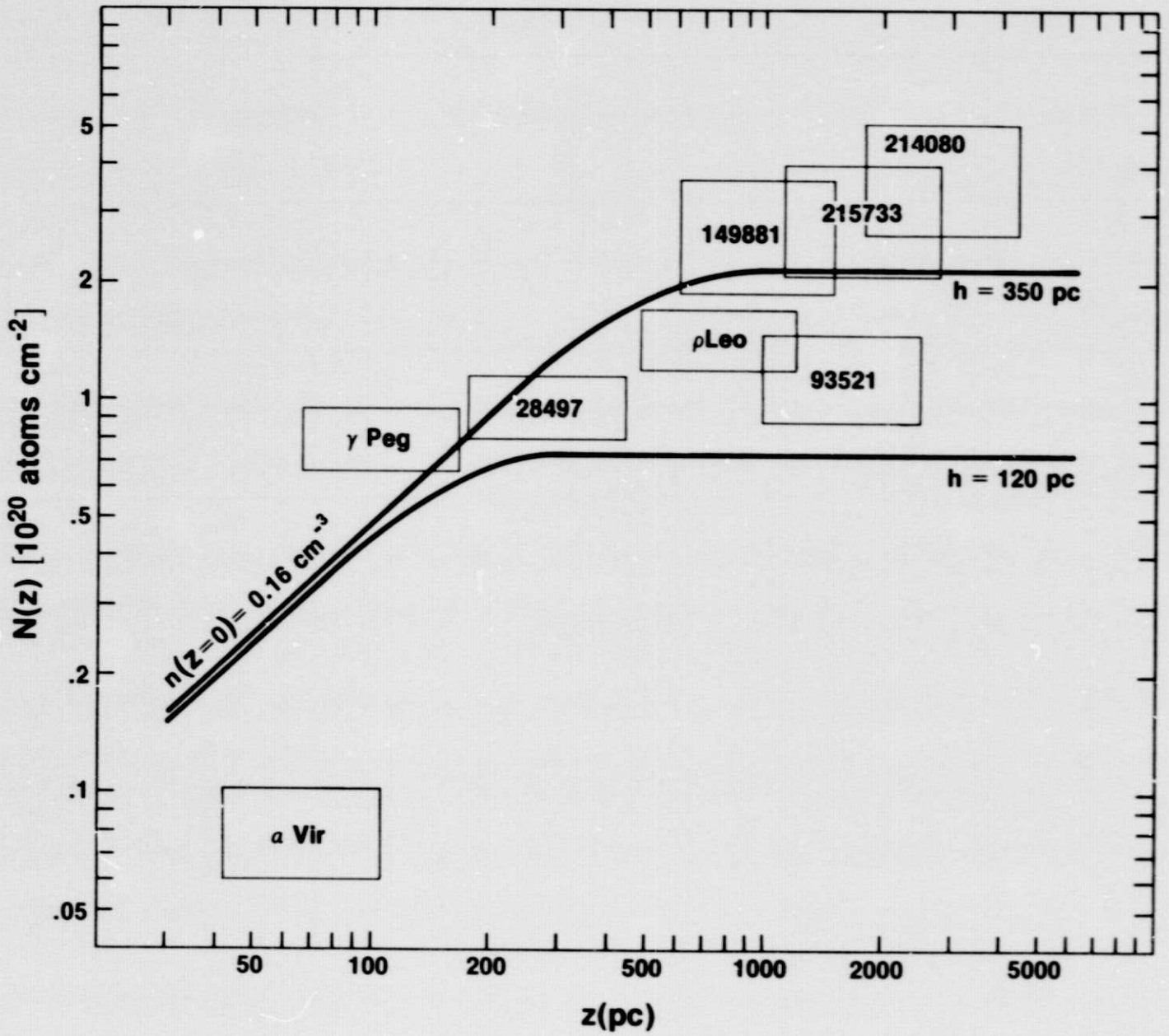
214080
215733
149881
h = 350 pc
ρLeo
93521
28497
γ Peg
h = 120 pc
n(z=0)= 0.16 cm-3
α Vir
N(z) [10^20 atoms cm^-2]
z(pc)
5
2
1
.5
.2
.1
.05
50
100
200
500
1000
2000
5000

Fig. 5